Physics Studies with Electron Cyclotron Resonance Heating and Current Drive on TEXTOR

E. Westerhof[1], A.J.H. Donné[1], J.A. Hoekzema[2], G.M.D. Hogeweij[1], V.F. Andreev[3], I.S. Bel'bas[3], M.F.M. de Bock[1], E. Farshi[1], K.H. Finken[2], R.J.E. Jaspers[1], H.R. Koslowski[2], A. Krämer-Flecken[2], A. Lazaros[1], X. Loozen[2], N.J. Lopes Cardozo[1], M.V. Maslov[3], A. Merkulov[1], K.A. Razumova[3], F.C. Schüller[1], R. Wolf[2], and TEC Team

1) FOM-Institute for Plasma Physics Rijnhuizen, Association EURATOM-FOM, PO Box 1207, 3430 BE Nieuwegein, The Netherlands, www.rijnh.nl*
2) Institut für Plasmaphysik, Forschungszentrum Jülich GmbH, EURATOM Association, D-52425 Jülich, Germany*
3) Nuclear Fusion Institute, RRC "Kurchatov Institute", 123182, Moscow, Russia

e-mail contact of main author: E.Westerhof@rijnh.nl

Abstract. The new 800 kW, 3 s, 140 GHz gyrotron has been applied on TEXTOR for physics studies with ECRH and ECCD. Slow magnetic field ramps demonstrate control of the sawtooth period: both co-ECCD and ECRH leading to long periods when positioned just outside the inversion radius, while counter-ECCD results in long sawtooth periods when positioned inside the inversion radius. Co-ECCD results in much shorter sawtooth periods when positioned inside the inversion radius. Switch-off of off-axis ECRH is seen to result in a transient improvement of confinement near the q=1 radius. This effect is observed to depend sensitively on both the position, power, and pulse length of ECRH. When properly localized at the q=2 surface, ECRH and ECCD are found to be capable to fully suppress the m=2, n=1 tearing modes induced by the Dynamic Ergodic Divertor.

1. Introduction

An active research programme on Electron Cyclotron Resonance Heating (ECRH) and Current Drive (ECCD) is being carried out on the TEXTOR tokamak. The main themes are the study and control of local electron transport and transport barriers and the control of instabilities like sawtooth oscillations and (neoclassical) tearing modes. First results were reported in Ref. [1]. This paper describes the advances in the ECRH system at TEXTOR, and in a number a high resolution electron diagnostics. The new 800 kW, long pulse (> 3 s), 140 GHz gyrotron in combination with the advanced diagnostics of Electron Cyclotron Emission-Imaging and multi-burst Thomson Scattering enabled a number of interesting physics studies that are reported as well. These physics studies include the manipulation of the current density profile near *q=1* by localized on and off-axis ECRH and ECCD both for control of sawteeth as well as for the creation of a transient transport barrier. In addition ECRH and ECCD have been used to study the suppression of m=2, n=1 tearing modes induced by the 2/1 side band perturbations of the Dynamic Ergodic Divertor (DED) [2,3].

2. Advances in the ECRH systems

A new high power (800 kW) and long pulse length (> 3 s), 140 GHz gyrotron (Gycom, Russia) has been brought into operation on the TEXTOR tokamak. Wave transmission to the tokamak is quasi-optical. The transmission line is screened by an aluminium enclosure. At strategic positions inside the enclosure, cooling water in Teflon hoses absorbs the stray radiation. The transmission line enters the TEXTOR hall via a dogleg labyrinth. The labyrinth

* Partners in the Trilateral Euregio Cluster

is lined with bricks and also serves as a long pulse, non-calorimetric power dump. The vacuum boundary at the tokamak is formed by a water-free fused silica window. Measurements indicate a temperature rise of 200 K in the central hot spot of this window during a full power, 1.5 s gyrotron pulse. From this temperature rise we estimate $\tan\delta = 1.8\ 10^{-4}$, corresponding to an absorption in the window of 2 %. Presently the last mirror is made of stainless steel (to limit eddy currents and disruption forces) with a copper insert that acts as a heat sink. Also the temperature rise of the last mirror is relatively small, indicating a surface reflectivity close to that of pure copper. Under these conditions, the applied gyrotron pulse length could be increased to 3 s at 800 kW. The tokamak window prevents further lengthening of the pulse length, while it also limits the duty cycle to only 1:1000. In 2005, it will be replaced by a water-cooled CVD diamond window.

3. Advances in high-resolution electron diagnostics

Two advanced electron diagnostics have recently been implemented onto TEXTOR. The first one is a burst-mode operated multipoint Thomson scattering system. Up to four bursts of about 5 ms long of laser pulses of 10 – 15 J each are extracted from an intra cavity ruby laser system [4] with a repetition rate of 10 kHz. The scattered light from either the full laser chord through the plasma (900 mm long) or from a 160 mm long part of the chord at the plasma edge is guided by fibre optics to a Littrow polychromator equipped with two fast CMOS cameras. First measurements with the Thomson scattering system that is still being commissioned, have concentrated on the observation of magnetic islands in DED-operated plasmas [5]. The second electron diagnostic is a microwave imaging system, combining a 128-channel ECE Imaging system, observing a matrix of 8 (radial) × 16 (vertical) points of about 1 cm^2 in the poloidal plane, and a 16-channel imaging reflectometer, observing about 12 cm of the cut-off surface at a single frequency of 88 GHz [6]. The ECE-I system is in routine use and has already delivered movies of the two-dimensional temperature evolution during a sawtooth precursor instability and subsequent crash. The imaging reflectometer, although still being commissioned, has yielded detailed information on the mode rotation velocity. The two imaging systems are operated fully simultaneously and can be used to diagnose the electron temperature and density fluctuations in the same plasma volumes.

4. Manipulation of the current density at *q=1*: effects on sawteeth and transport

The current density evolution near the *q=1* surface has been manipulated by on- and off-axis ECRH and ECCD in order to control both the sawtooth behaviour and the plasma transport. Dynamic magnetic field scans of counter-ECCD show a strong lengthening of the sawtooth period when the power deposition (ρ_{dep}) is localised well inside the sawtooth inversion radius (ρ_{inv}). For $\rho_{dep} > \rho_{inv}$, counter-ECCD does not change the sawtooth period. In contrast, sawtooth stabilisation by co-ECCD and ECRH requires deposition at or just outside the inversion radius. The results of three discharges with slow dynamic magnetic field ramps during a long ECRH, co, or counter-ECCD pulse are shown in Fig. 1. There are no indications that the sawtooth inversion radius ($r_{inv}/a \approx 0.25$) changes strongly during these experiments.

In case sawteeth are stabilised by off-axis ECRH, a transient internal transport barrier is sometimes observed after switch-off of ECRH, which results in a delayed decay of the central electron temperature, while at the same time the temperature outside the inversion radius decreases rapidly (see Fig. 2). The duration of the phase in which the core electron temperature stays constant can be as long as 35 ms. This effect was previously observed on T-10 [7]. The experimental data cannot be explained when it is assumed that the electron

thermal transport stays constant (see Fig. 2). Whether or not the effect is observed depends critically on the local magnetic shear in the vicinity of the q=1 rational surface, which should be close to zero. In that case an internal transport barrier is induced, leading to a decrease of the electron thermal diffusivity χ_e [8], as has been calculated with the COBRA code [9] (see Fig. 3).

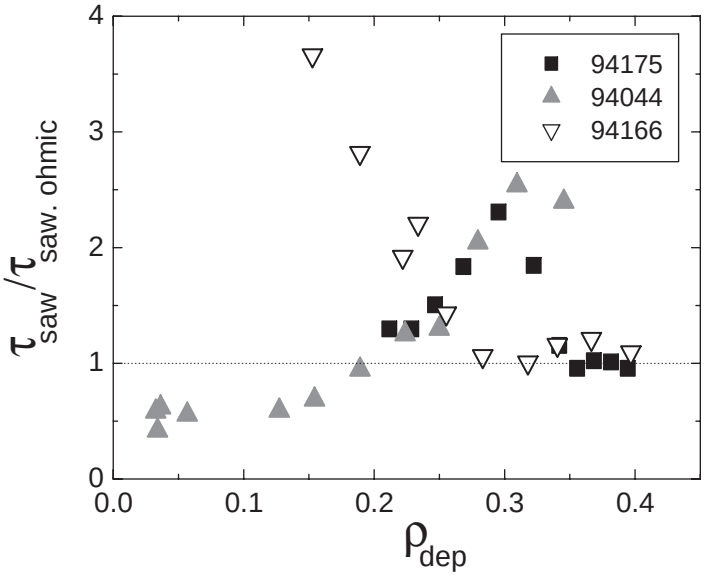

Fig. 1 The sawtooth period normalised to the ohmic sawtooth period is shown for three discharges as a function of the normalized deposition radius ρ_{dep}, which is changed during ECRH/ECCD by a slow B_T ramp down. The toroidal injection angle in the three discharges is perpendicular (#94175) for ECRH, and –20° (#94044) or +10° (#94166) off-perpendicular for co- and counter-ECCD, respectively

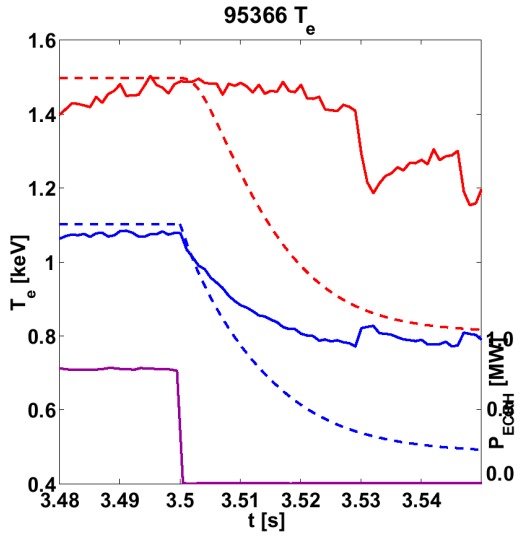

Fig. 2. Observed (full) and calculated (dashed) T_e evolution after ECRH switch-off assuming that the electron thermal transport is not modified. The top, red curve represents $T_e(0)$ and the blue curve gives T_e just outside ρ_{dep}.

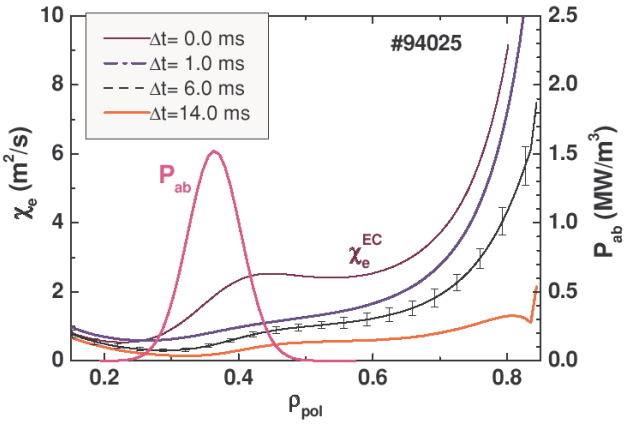

Fig.3. COBRA calculation of χ_e during ECRH and at various time slices after ECRH switch-off at Δt = 0 ms.

5. Study and suppression of error field induced tearing modes by ECRH and ECCD

When the DED is operated to create a dominant m=3, n=1 magnetic field perturbation also a strong m=2, n=1 side band is produced. Above a certain threshold, the latter is observed to create a large 2/1 magnetic island in the plasma [3], which is locked to the DED perturbation. These islands are very clearly seen on the multipoint Thomson scattering system. In particular in case of DC operation of the DED, when all pulses from a single burst can be summed to improve the photon statistics (Fig. 4) [5].

Modulated ECRH has been used to study the changes in transport during plasma operation with DED above threshold for 2/1 mode generation. As illustrated in Fig. 5 by the phase and amplitude response of the electron temperature from ECE to Modulated ECRH, the transport is increased not just around the magnetic islands created by the DED, but over most of the cross-section. Simulations of the propagating heat pulses show that for both cases the incremental heat diffusivity (χ_e^{inc}) outside ρ_{dep} is much higher than inside ρ_{dep}. For the discharges shown in Fig. 4, the increase of χ_e^{inc} due to the presence of the 2/1 island is about a factor of 4 inside ρ_{dep} (χ_e^{inc} increasing from ~0.8 to ~3.2 m^2/s), and a factor of 2 outside ρ_{dep} (χ_e^{inc} increasing from ~6 to ~12 m^2/s).

Also the suppression of the DED induced m=2, n=1 tearing modes by localized ECRH or ECCD has been studied. A reproducible target discharge was set up, with a toroidal field of B_T = 2.25 T, plasma current I_p = 300 kA, and 300 kW of NBI for diagnostic purposes (CXRS, MSE). The DED is then operated in its AC mode at 1 kHz with a maximum current of 2 kA in each coil, well above threshold for triggering of the m=2, n=1 tearing mode at the q=2 surface at approximately mid radius, $\rho_{q=2} \approx 0.5$ [3]. For these parameters the cold EC resonance is located at a major radius just inside the q=2 surface on the high field side, and the ECRH deposition has been varied by changing the vertical injection angle. ECRH is then applied in the flat top phase of the DED to study its effect on the 2/1 mode. A relative estimate of the amplitude of the 2/1 mode is obtained from the 1 kHz fluctuations of the 141 GHz ECE originating from close to the q=2 surface, and from the 1 kHz fluctuations on different Mirnov coils on the low field side of the vacuum vessel (opposite the DED coils).

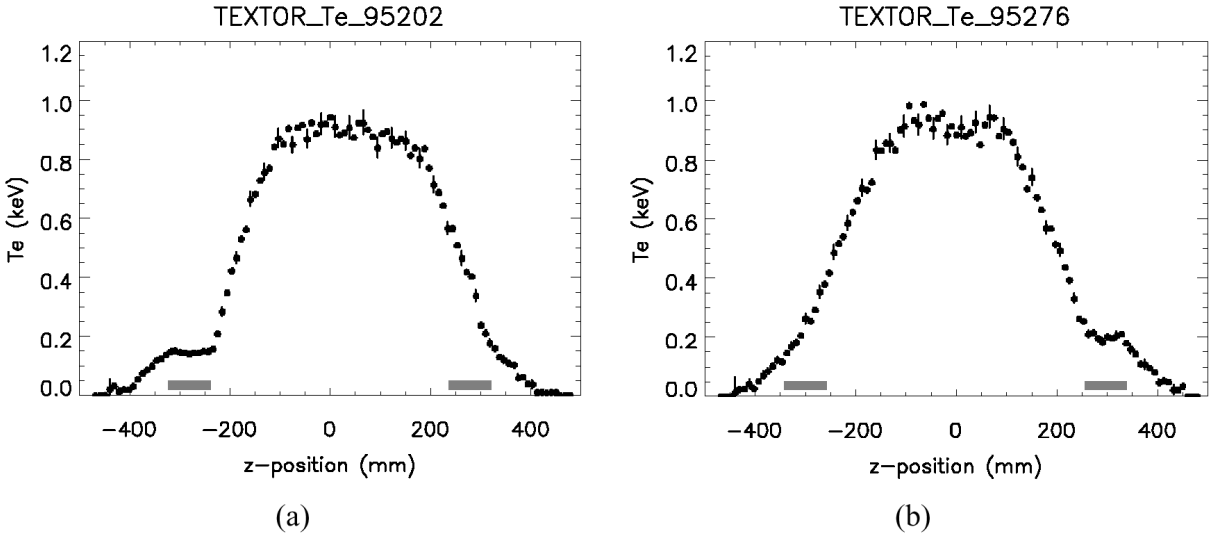

Fig. 4 Temperature profiles obtained from summing all 14 pulses from a single burst of the multipoint Thomson scattering system through different positions of a large island, measured in two different DC-DED shots. The m=2 island structures positioned around ±30 cm having size of ~8 cm (depicted by grey areas) are clearly seen in both shots. The profile perturbation by the islands is asymmetric and is consistent with the DED coil settings [5].

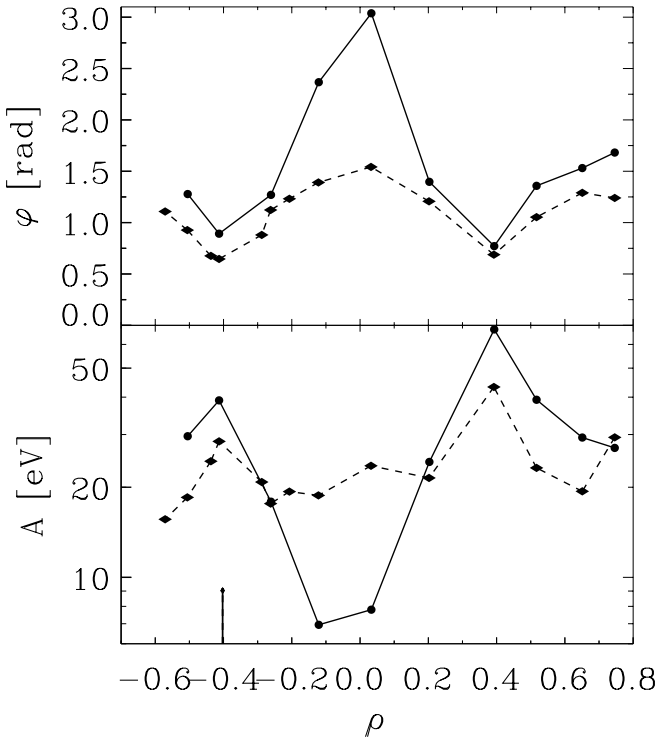

Fig. 5 Phase (ϕ) and amplitude (A) of temperature fluctuations in response to MECH. Full: without DED perturbation. Dashed: with DED perturbation above threshold for the 2/1 mode.

The discharge scenario for these tearing mode control experiments is illustrated in Fig. 6. The figure clearly shows the sudden drop in plasma rotation as the DED m=2, n=1 perturbation field penetrates and a 2/1 magnetic island which is locked to the 1 kHz DED perturbation is created. This coincides with the increase in the fluctuations on the 141 GHz ECE intensity coming from close to the q=2 surface and in the fluctuations on the Mirnov coils. When ECRH is applied both the ECE and the Mirnov fluctuations are strongly suppressed, while also the plasma rotation slightly recovers. Figure 7 shows the rate of mode suppression, $\widetilde{T}_{ECRH} / \widetilde{T}_{DED}$, as a function of the normalised deposition radius, ρ_{dep}, for two series of discharges with ECRH, and co-ECCD, respectively. In case of ECRH the normalised width (FWHM) of the deposition profile is $\Delta\rho_{dep} = 0.02$. Co-ECCD is affected by selecting a toroidally oblique injection angle of -15^{o}. A linear adjoint calculation [10] predicts a driven current of about 8 kA, with a deposition profile width of $\Delta\rho_{dep} = 0.07$. Almost complete mode suppression is obtained for full power (800 kW) ECRH or co-ECCD located precisely at the position of q=2. As can be seen in Fig. 6, co-ECCD is slightly more effective for mode suppression than ECRH only. In the co-ECCD case, the broader deposition profile also results in a proportionally broader range over which the mode is suppressed. The discharges at the edges of the deposition scans all ended in disruptions as the plasma was further destabilised by the ECRH (in spite of the partial stabilization of the 2/1 mode). The strong increase in mode activity indicated for heating well inside the q=2 surface (#94722 in Fig. 7) on the ECE oscillations is not confirmed by the Mirnov coils, and in this case is most likely due to an increase in the temperature gradient at the q=2 surface rather than an increase in the magnetic island size. A power scan for both ECRH, and co-ECCD at the optimum ρ_{dep} shows that in both cases the maximum available power of 800 kW is only marginally sufficient for stabilization of the mode.

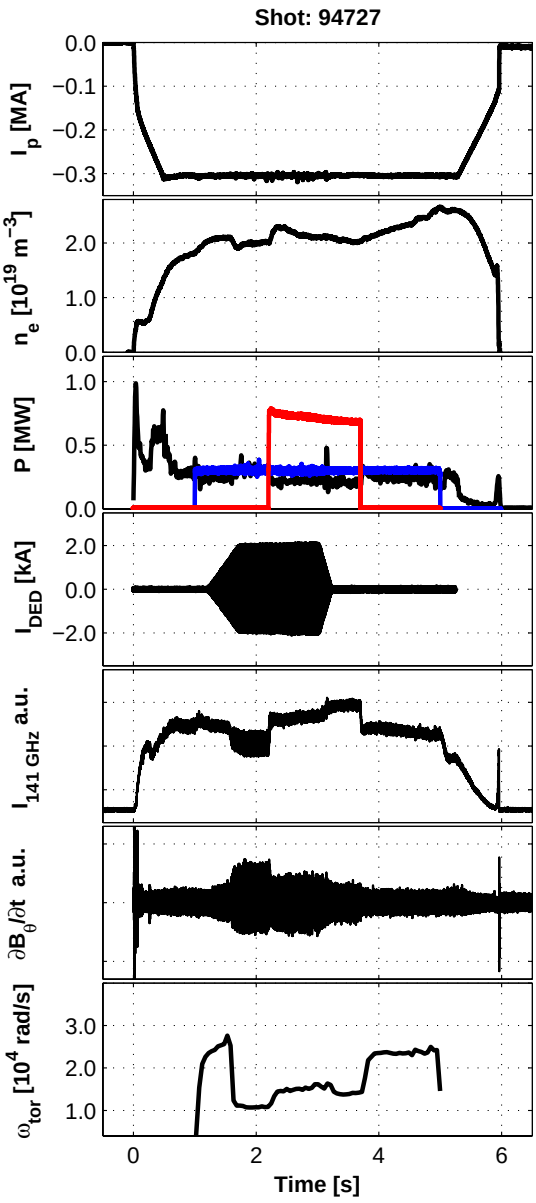

Fig. 6 The discharge scenario for the tearing mode suppression experiments. The panels show from top to bottom: the plasma current; the central line integrated density; the ohmic (black), neutral beam (blue), and ECRH (red) powers; the DED current; the 141 GHz ECE intensity; a Mirnov coil signal; the central plasma toroidal rotation derived from active charge exchange recombination spectroscopy.

The penetration of the 2/1 DED perturbation field is signalled by the sudden drop in the plasma rotation and the coincident increase in the fluctuations on the 141 GHz ECE coming from close to the q=2 surface and in the fluctuations on the Mirnov coils. When ECRH is applied both the ECE and the Mirnov fluctuation are strongly suppressed, while also the plasma rotation slightly recovers.

ECRH/ECCD has been operated under feedback control from the DED current: the gyrotron power is modulated in phase with the rotation of the DED magnetic perturbation and, consequently, in phase with the locked 2/1 magnetic island. ECRH power is switched between high, 800 kW and low power, 150 kW with a 50% duty cycle. The phase between the DED current and the ECRH power modulation has been varied in order to scan the ECRH power deposition through the magnetic island. Figure 8 shows the results obtained with modulated heating and current drive at the optimum ρ_{dep} for mode suppression. Here ECRH and co-ECCD are seen to be most effective when injected in phase with the magnetic island O-points. However, the efficiency of mode suppression of modulated ECRH or co-ECCD is very similar to that of continuous ECRH and co-ECCD at the maximum power, although the time averaged power of the modulated ECRH/ECCD is obviously lower.

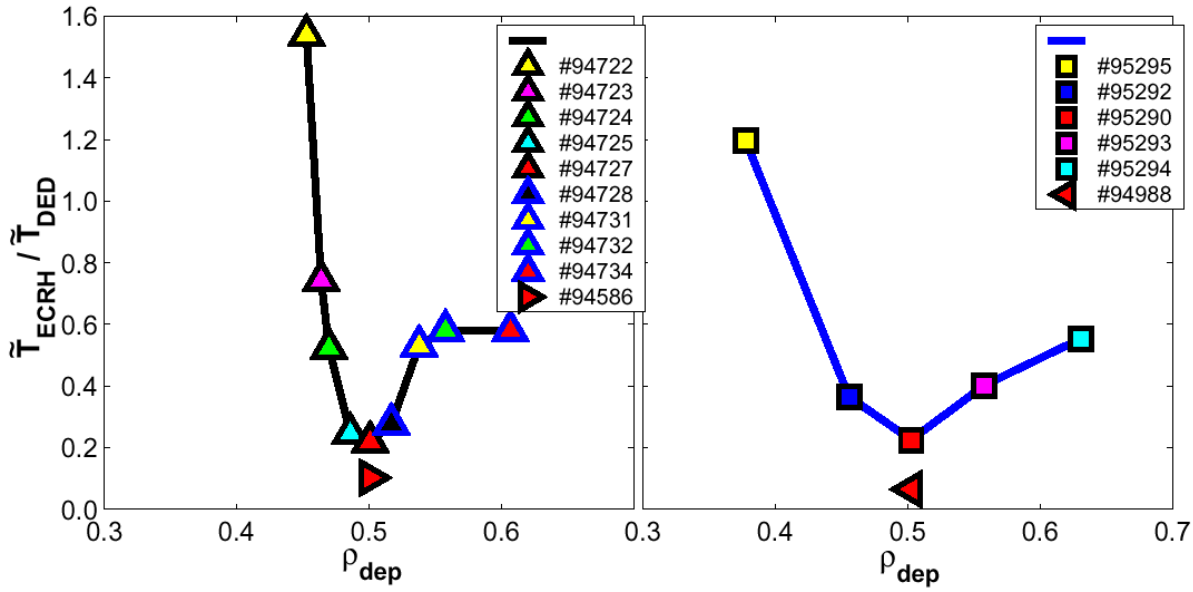

Fig. 7 The suppression rate of the m=2, n=1 tearing mode as a function of the ECRH (left) and ECCD (right) deposition radius. The latter has been varied by changing the vertical injection angle. The vertical angle is converted into a normalised deposition radius by ray-tracing, which does however not yet account for the proper Shavranov shift and must be regarded as approximate. A relative measure of the 2/1 island size is obtained from the amplitude of the 1 kHz oscillations on the 141 GHz ECE originating from close to the q=2 surface. The figure shows the ratio of the 1 kHz oscillations during ECRH (ECCD) over those in the presence of the DED generated island alone. These results are in qualitative agreement with the measurements from Mirnov coils on low field side of the tokamak.

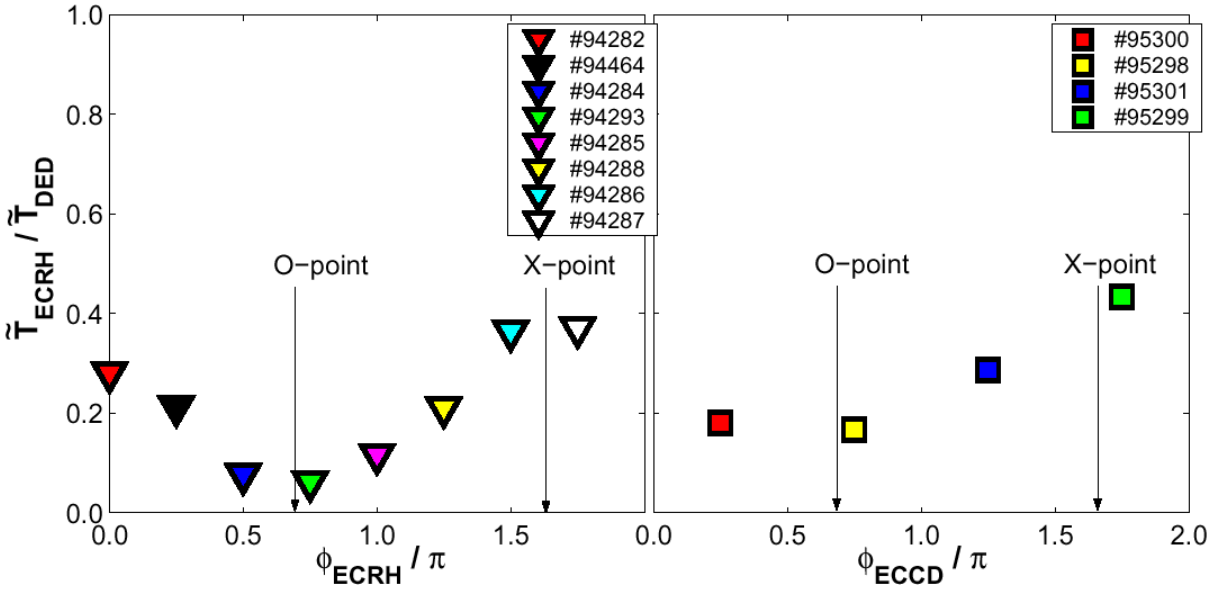

Fig. 8 The suppression rate of the m=2, n=1 tearing mode obtained from the 1 kHz oscillations on the 141 GHz ECE originating from close to the q=2 surface is shown as a function of the phase of the high power ECRH (left) or ECCD (right) relative to the current in one of the DED coils. For these experiments, the ECRH/ECCD power has been modulated with a 50% duty cycle between a high (~780 kW) and a low (~180 kW) power level phase locked to one of the DED coil currents. The arrows indicate where the phasing is such that in the middle of the high power ECRH/ECCD phase the power deposition coincides with the O-point or X-point of the magnetic island.

6. Summary and Conclusions

The new 800 kW, 3 s, 140 GHz gyrotron has been used for a variety of physics studies with ECRH and ECCD on TEXTOR. Slow magnetic field ramps have been performed to study sawtooth control. Both co-ECCD and ECRH are seen to result in increased sawtooth periods when positioned just outside the inversion radius, while counter-ECCD increases the sawtooth period when positioned inside the inversion radius. Co-ECCD decreases the sawtooth period when positioned inside the inversion radius. Switch-off of off-axis ECRH is seen to result in a transient improvement of confinement near the q=1 radius. This effect, previously observed on T-10 [6], is observed to depend sensitively on both the position and pulse length of ECRH. This can be understood by the critical role played by the shear near the q=1 surface, which should be close to zero for the effect to occur. Finally, the suppression of m=2, n=1 tearing modes induced by the 2/1 side band of the perturbation field of the Dynamic Ergodic Divertor (DED) at TEXTOR has been studied. When properly localized at the q=2 surface, ECRH and ECCD are found to be capable to fully suppress these m=2, n=1 tearing modes induced by the DED. Similar efficiencies are obtained for continuous ECRH (ECCD) or modulated ECRH (ECCD) phased properly around the island O-point. Modulated ECRH (ECCD) phased around the X-point is, however, far less efficient than modulated ECRH phased around the O-point.

Acknowledgements

This work, supported by the European Communities under the contract of Association between EURATOM/FOM, was carried out within the framework of the European Fusion Programme. The views and opinions expressed herein do not necessarily reflect those of the European Commission.

References

[1] WESTERHOF, E. et al., Nucl. Fusion **43** (2003) 1371.
[2] Special Issue, Fusion Eng. Design **37** (1997) 335.
[3] KOSLOWSKI, H.R., et al., 31st EPS Conf. London (2004), ECA, Vol **28G**, P1-124.
[4] VAN DER MEIDEN, H.J., et al., Rev. Sci. Instrum. **75** (2004)
[5] VARSHNEY, S.K., et al., Proc. 31st EPS Conf. London (2004), ECA, Vol **28G**, P1-127.
[6] PARK, H.K., et al., Rev. Sci. Instrum. **75** (2004)
[7] RAZUMOVA, K.A., et al., Plasma Phys. Control. Fusion **45** (2003) 1247
[8] HOGEWEIJ, G.M.D., et al, 31st EPS Conf. London (2004), ECA, Vol **28G**, P1-119.
[9] ANDREEV, V.F., et al, Plasma Phys. Control. Fusion **46** (2004) 319.
[10] COHEN, R.H., Phys. Fluids **30** (1987) 2442 and **32** (1988) 421.